



A Triple-Network Dynamic Connection Study in Alzheimer's Disease

Xianglian Meng¹, Yue Wu¹, Yanfeng Liang², Dongdong Zhang², Zhe Xu¹, Xiong Yang¹ and Li Meng^{3*}

¹ School of Computer Information and Engineering, Changzhou Institute of Technology, Changzhou, China, ² School of Basic Medical Sciences, Jiamusi University, Jiamusi, China, ³ School of Physics, Engineering and Computer Science, University of Hertfordshire, Hatfield, United Kingdom

OPEN ACCESS

Edited by:

Zhuqing Jiao,
Changzhou University, China

Reviewed by:

Xiaohui Zhan,
Chongqing Medical University, China
Yanfeng Zhao,
Shandong University of Science and
Technology, China

*Correspondence:

Li Meng
l.1.meng@herts.ac.uk

Specialty section:

This article was submitted to
Computational Psychiatry,
a section of the journal
Frontiers in Psychiatry

Received: 26 January 2022

Accepted: 21 February 2022

Published: 04 April 2022

Citation:

Meng X, Wu Y, Liang Y, Zhang D,
Xu Z, Yang X and Meng L (2022) A
Triple-Network Dynamic Connection
Study in Alzheimer's Disease.
Front. Psychiatry 13:862958.
doi: 10.3389/fpsy.2022.862958

Alzheimer's disease (AD) was associated with abnormal organization and function of large-scale brain networks. We applied group independent component analysis (Group ICA) to construct the triple-network consisting of the saliency network (SN), the central executive network (CEN), and the default mode network (DMN) in 25 AD, 60 mild cognitive impairment (MCI) and 60 cognitively normal (CN) subjects. To explore the dynamic functional network connectivity (dFNC), we investigated dynamic time-varying triple-network interactions in subjects using Group ICA analysis based on k-means clustering (GDA-k-means). The mean of brain state-specific network interaction indices (meanNII) in the three groups (AD, MCI, CN) showed significant differences by ANOVA analysis. To verify the robustness of the findings, a support vector machine (SVM) was taken meanNII, gender and age as features to classify. This method obtained accuracy values of 95, 94, and 77% when classifying AD vs. CN, AD vs. MCI, and MCI vs. CN, respectively. In our work, the findings demonstrated that the dynamic characteristics of functional interactions of the triple-networks contributed to studying the underlying pathophysiology of AD. It provided strong evidence for dysregulation of brain dynamics of AD.

Keywords: Alzheimer's disease, large-scale brain networks, triple-network, functional connectivity, dynamic cross-network interaction

INTRODUCTION

As a neurodegenerative disease, Alzheimer's disease (AD) has an irreversible pathology, a long course of disease, and a progressive aggravation (1). Although the relationship between mild cognitive impairment (MCI) and AD is still inconclusive, some researchers believe that MCI is a transition period between normal aging and AD (2). Many studies report that cognitive decline and preclinical stages of impairment in AD are primarily due to disruption of brain networks. The episodic memory and executive functions of AD appear to be abnormal, and the related functions are closely related to the normal functioning and integrity of the brain network. Most of the brain networks involved in AD research are: default mode network (DMN), central execution network (CEN), and salience network (SN). The changes of DMN, CEN, and SN may be related to the

pathological changes of AD (3–6). For example, important areas of the DMN are closely related to memory, among which the medial temporal cortex and hippocampal memory are strongly correlated. Research has shown that DMN exhibits functional connectivity disruption in AD (6, 7). Dennis et al. found that functional connectivity and network integrity decline gradually during normal aging, but decline more rapidly in AD patients, with the greatest impact on DMN (8). The main component of the SN is the inferior frontal cortex, which is closely related to cognitive function and plays an important role in cognitive control (9). CEN is a brain network implicated in human cognitive control, and its frontal regions are implicated in episodic memory. The nodes of the CEN include the dorsolateral prefrontal cortex and the lateral posterior parietal cortex. The study of CEN is helpful for the monitoring of brain network in MCI patients (10).

Functional Magnetic Resonance Image (fMRI) is a non-invasive brain imaging technology with high spatiotemporal resolution and good repeatability. More and more applications in the field of brain science. Resting-state fMRI(rs-fMRI) is the data obtained when the subject lies in the magnetic resonance scanner without any stimulation and task processing. Compared with the task state, the research subject's coma, anesthesia and other states are also included. In the resting state, the brain also has inherent neural activity patterns and can perform specific functions. It is of great significance to use rs-fMRI to study the topology of the brain network. The advent of fMRI has brought about a growing number of methodological tools for studying cognitive function and dysfunction (11–14). Effectively separating meaningful neural signals from fMRI images and constructing brain functional network has important research significance for its earlier disease prediction. However, most studies mainly use static functional connectivity (sFC) from fMRI. Large-scale dynamic functional network connectivity (dFNC) provides more context-sensitive, dynamic, and direct view at higher network level. It distinguishes brain network dynamics between normal and diseased populations (5, 13, 15–18). The characteristics of dFNC data are that time is constantly changing, reflecting brain activity that changes over time, and different functional connectivity networks can be obtained at different moments, in sharp contrast to sFC. Menon proposed a triple network model consisting of the DMN, SN and (19). Many studies have demonstrated that the dynamic interactions among triple-network (DMN, SN, CEN) are critical for complex cognitive tasks. These contribute to early recognition of Alzheimer's disease (6, 12, 20–24).

Independent Component Analysis (ICA) is a method based on data analysis, without a priori assumptions, it can separate and extract the physiological noises such as head movement, heartbeat and breathing in the BOLD signal, while the brain activity-related components can be separated and extracted. Signal components can form a network of related functional brain areas, which is an increasingly widely used data analysis method in rs-fMRI research (25). Although the components extracted by the ICA method have good reproducibility and reliability, the traditional ICA method applied to individual fMRI data

cannot extract the common characteristics among a group of subjects (26). The Group Independent Component Analysis (Group ICA) method is based on the traditional independent component analysis, through the fusion of independent components across individuals, to construct a group independent component, thus reflecting the overall characteristics of the brain operating mechanism of a group of subjects (27).

In our work, we employed Group ICA to construct the triple-network (CEN, SN, and DMN) in AD, MCI and cognitively normal (CN). Then, we performed dFNC analysis of the three groups (MCI-AD-CN). Finally, we used statistical analysis and support vector machine (SVM) to validation. The study workflow was shown in **Figure 1**.

MATERIALS AND METHODS

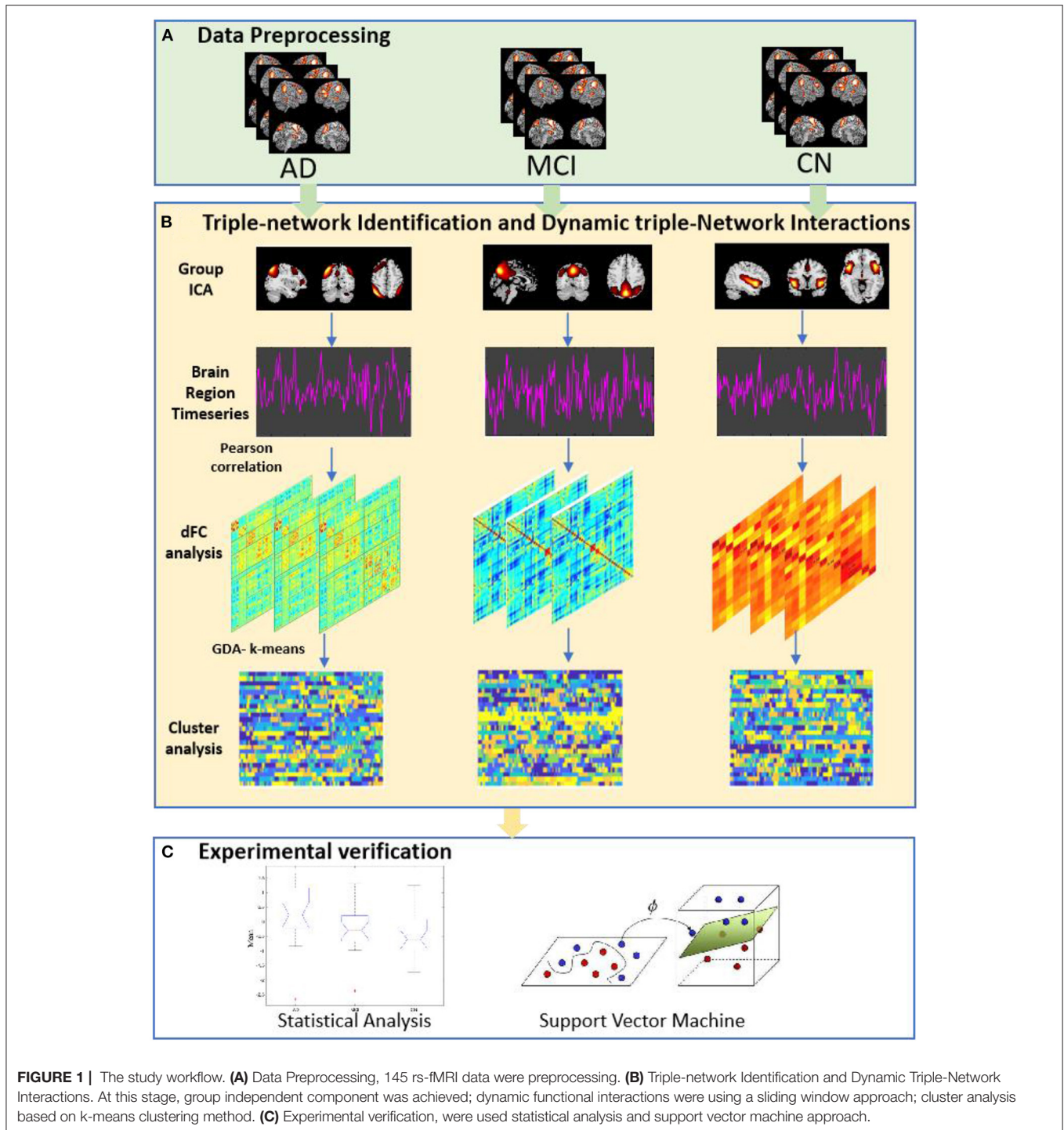
Subjects

The data for our study were obtained from the Alzheimer's Disease Neuroimaging Initiative (ADNI) database (www.adni-info.org). ADNI was established in 2003 at the initiative of Principal Investigator Michael W. Weiner, and was funded by the National Institutes of Health Security and the National Center for Aging Health and more than 20 private companies. It was designed to aid in the diagnosis of AD by using data including clinical diagnosis, neuroimaging, genetic material, and biomarkers. ADNI studies were conducted in ADNI-1, ADNI-GO, ADNI-2, and ADNI-3 phases. After three phases of research, the ADNI dataset has collected multiple multimodal data including MRI, PET, blood biomarkers, cerebrospinal fluid biomarkers (A β , tau protein) and genetic material. MRI was considered the preferred neuroimaging examination for AD. MRI data in the ADNI dataset were divided into three categories: AD, MCI, and CN subjects (28). fMRI was primarily measured by the relative levels of deoxyhemoglobin in each voxel, and rs-fMRI was to let the subject's brain completely empty, and to observe the characteristics of the interconnection of nerve fibers in the brain state without special activity (29).

In our study, rs-fMRI data ($N = 145$) included 60 cognitively normal (CN), 60 Mild Cognitive Impairment (MCI) and 25 AD subjects. The characteristics of the used subjects were shown in **Table 1**. The table showed that there were significant differences among the three groups in terms of gender ($p < 0.001$), age ($p < 0.001$), and MMSE ($p < 0.001$).

Data Preprocessing

MRI is one of the most commonly used methods for AD auxiliary diagnosis. MRI is divided into T1 and T2, where T1 is used to observe anatomical structures, T2 is used to display the lesion tissue. In this study, T1 is used as a reference image to which rs-fMRI data can be registered. The rs-fMRI ($64 \times 64 \times 48$) were obtained using an echo-planar imaging (EPI) sequence. Data preprocessing process: (1) Convert rs-fMRI from DICOM



format to Nifti format using MRIcro software [MRIcro software guide (sc.edu)]. (2) We use SPM12 (30) and DPABI (31) for preprocessing as follows: (1) Remove the first 10 time points, Time points is set to 187, TR is set to 3 s; (2) Slice timing correction (slice number = 48, Reference slice = 48); (3) Realign and normalize: the MRI image of each subject is registered to the MNI standard space, and the volume distribution map of

the brain gray matter is obtained after processing, and then the gray matter volume image of the registered standardized image is resampled to calculate $3 \times 3 \times 3 \text{ mm}^3$ relative gray matter volume map ($61 \times 73 \times 61$); Normalize by DARTEL; (4) Smooth by using FWHM (full width at half maximum) of $8 \times 8 \times 8 \text{ mm}^3$; (5) Band-pass filtering with 0.01~0.1 Hz; (6) Standardized settings: polynomial trend, frist on 24 head

TABLE 1 | The clinical characteristics of subjects.

Subjects	CN	MCI	AD	P
Number	60	60	25	-
Gender (M/F)	17/43	29/31	14/11	<0.001
Age (mean ± sd)	72.7 ± 7.3	76 ± 8.5	76.7 ± 9.1	<0.001
MMSE (mean ± sd)	28.9 ± 1.3	27 ± 2.2	21.1 ± 3.9	<0.001

CN, Cognitively Normal; MCI, Mild Cognitive Impairment; AD, Alzheimer’s disease; MMSE, Mini mental status examination. T-tests were used for gender, age, and MMSE.

motion parameters, white matter signal, and cerebrospinal fluid signal.

Triple-Network Identification Group Independent Component Analysis

In our study, we employed group independent component analysis (Group ICA) to construct the triple-network (DMN, SN, and CEN). The principle of Group ICA was as follows: multiple subjects were compressed into fractions by principal component analysis (PCA) and then concatenated, the concatenated data was again reduced by PCA to reduce the fractions, and finally the mixed data was extracted by ICA to separate independent components. We set the ICA components to 30.

The mixed data of M subjects were reduced to the number of components by PCA, as shown in Formula 1.

$$\bar{x}^{(m)} = \left(F^{(m)}\right)^{-1} x^{(m)}, 1 \leq m \leq M \tag{1}$$

Where $\bar{x}^{(m)}$ is the matrix of $L \times V$ after dimensionality reduction, $x^{(m)}$ is the original mixture matrix of $T \times V$, $\left(F^{(m)}\right)^{-1}$ is the dimensionality reduction matrix of $L \times T$, T and V are the number of time points and voxels of the data, and L is the time after dimensionality reduction dimension.

Then, we concatenated all the data after dimensionality reduction and used further dimensionality reduction as in Formula 2.

$$X = Q^{(-1)} \times \begin{bmatrix} \bar{x}^{(1)} \\ \bar{x}^{(2)} \\ \vdots \\ \bar{x}^{(M)} \end{bmatrix} = Q^{(-1)} \times \begin{bmatrix} \left(F^{(1)}\right)^{-1} x^{(1)} \\ \left(F^{(2)}\right)^{-1} x^{(2)} \\ \vdots \\ \left(F^{(M)}\right)^{-1} x^{(M)} \end{bmatrix} \tag{2}$$

where $Q^{(-1)}$ is the dimensionality reduction matrix of $N \times LM$. After two PCA dimensionality reduction, the ICA algorithm was used to extract independent components. The ICA algorithm model was shown in Formula 3.

$$X = \hat{A}\hat{s} \tag{3}$$

where \hat{A} is the mixture matrix of $N \times N$, and \hat{s} is the matrix of $N \times V$ to represent N independent source signals.

Finally, it was reconstruction, using the estimated mixing matrix and source signal to reconstruct the time series and spatial images of M subjects, then the reconstructed source signal was as in Formula 4.

$$\hat{S}^{(m)} = \left(\hat{A}^{(m)}\right)^{-1} \left(Q^{(m)}\right)^{-1} \times \left(F^{(m)}\right)^{-1} x^{(m)} \tag{4}$$

We employed GIFT toolkit (<http://icatb.sourceforge.net/>) for Group ICA (32, 33). We identified the DMN, SN, left CEN, and right CEN in 145 subjects.

The Analysis of DFNC

After extracting the BOLD time series of all ROIs of the subject, an exponentially decaying (ED) sliding-window strategy was applied to construct the dFNC of the brain. In this study, a sliding window of length N was selected, and the time series of length L was divided into T overlapping subsequences according to a certain step size s , where $T = (L - N)/s + 1$, then calculated the FNC matrix corresponding to each window.

The ED weights are computed as Formula 5.

$$w_t = w_0 e^{(t-T)/\theta}, t = 1, \dots, T, \tag{5}$$

where $w_0 = (1 - e^{-1/\theta})/(1 - e^{-T/\theta})$, t is the t^{th} time point within the sliding window, T is the sliding window length (12), and the parameter θ controls the influence from distant time points. θ is set to a third of the window length (34). We set T to 39 s (TRs = 3 s) and sliding step to 1 s (35).

The definition of edge in brain network research was the functional connection between two brain regions. The dFNC between the two brain regions was determined by weighted Pearson correlation (wPC). It can reflect the interaction with time series of any two nodes x_t and y_t as Formula 6.

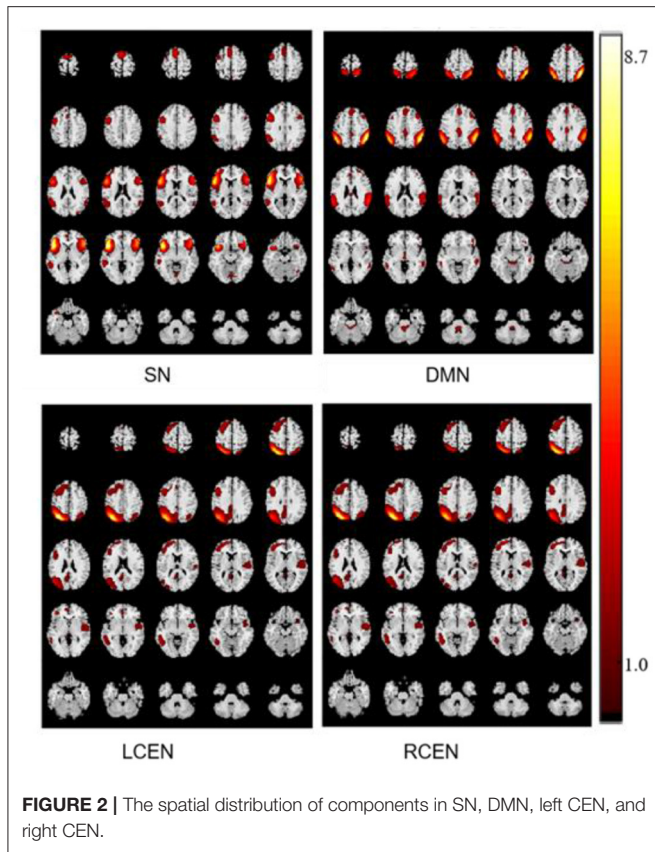
$$r_w = \frac{\sum_{t=1}^T w_t (x_t - \bar{x})(y_t - \bar{y})}{\sqrt{\sum_{t=1}^T w_t (x_t - \bar{x})^2} \sqrt{\sum_{t=1}^T w_t (y_t - \bar{y})^2}} \tag{6}$$

where $\bar{x} = \frac{\sum_{t=1}^T w_t x_t}{T}$ and $\bar{y} = \frac{\sum_{t=1}^T w_t y_t}{T}$, then we calculated the z-transform of the weighted Pearson correlation.

Dynamic Triple-Network Interactions

To make the clustering results independent of the number of subjects, 25 subjects with no significant differences in age and gender were selected from each group for cluster analysis. We explored group difference analysis based on k-means clustering method (GDA- k-means) (36).

The lower triangle (i.e., the six contiguous edges that do not repeat) of the weighted dynamic connectivity matrix M of 4×4 of each subject was extracted to form the data set D , $D = \{m_1, m_2, \dots, m_x\}$. Afterwards, the functional connectivity matrix M of each group of subjects was clustered individually by using k-means. Since the distance function was not specified in the citation, the default Euclidean distance was used for the



distance calculation, and the optimal number K of clusters was found using the silhouette maximum method (37), which finally C divided the sample set into K clusters. The process of clustering was as follows, firstly, k samples were randomly selected from the dataset D as the initial k prime vectors, which represented as $\mu = \{\mu_1, \mu_2, \dots, \mu_k\}$ C initialize the final cluster division as $C_t = \varphi, (t = 1, 2, \dots, k)$. After that, the samples x_i and each center-of-mass vector were taken to μ_j calculate the Euclidean distance d_{ij} , which was calculated as shown in Formula 7.

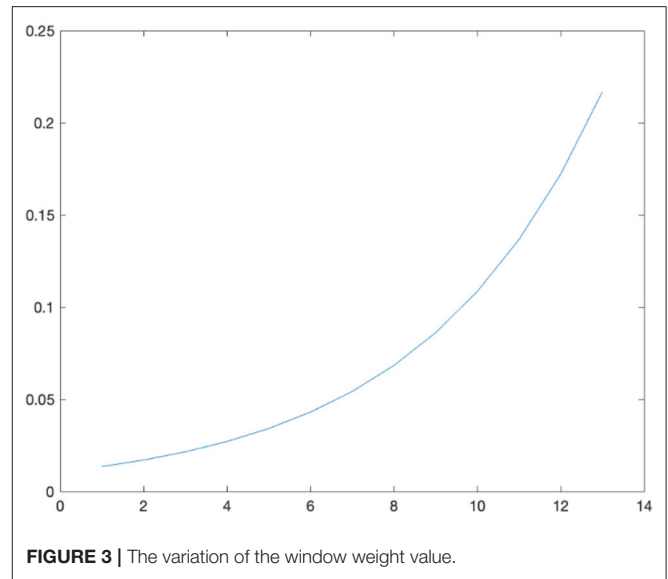
$$d_{ij} = \sqrt{(m_i - \mu_j)^2} \tag{7}$$

The corresponding class corresponding to the x_i smallest d_{ij} fetch was noted as λ_i and the sample clusters were updated $C_{\lambda_i} = C_{\lambda_i} \cup \{x_i\}$. The above clustering steps were repeated and the sample clusters $C = \{C_1, C_2, \dots, C_K\}$ are finally output.

For each subject, we calculated the mean lifetime of each brain state based on the average time spent consecutively. We employed the brain state-specific network interaction index (NII) (9, 38) to characterize DMN, SN, and CEN network interactions (7).

The NII is calculated as shown in Formula 8.

$$NII = f(PC_{SN,CEN}) - f(PC_{SN,DMN}) \tag{8}$$



where

$$f(PC) = \frac{1}{2} \ln\left(\frac{1 + PC}{1 - PC}\right) \tag{9}$$

PC is Pearson's correlation between the time series of two networks, such as $PC_{SN,DMN}$ refers to correlation between the time series of SN and DMN. $f(PC)$ computes Fisher z-transform of Pearson Correlation (PC) between ROI time series. That is, the fisher-z changes of the functional connectivity coefficients of SN-LCEN and SN-RCEN were summed and subtracted from the fisher-z changes of the functional connectivity coefficients of SN-DMN.

The Classification Based on Dynamic Triple-Network Interactions

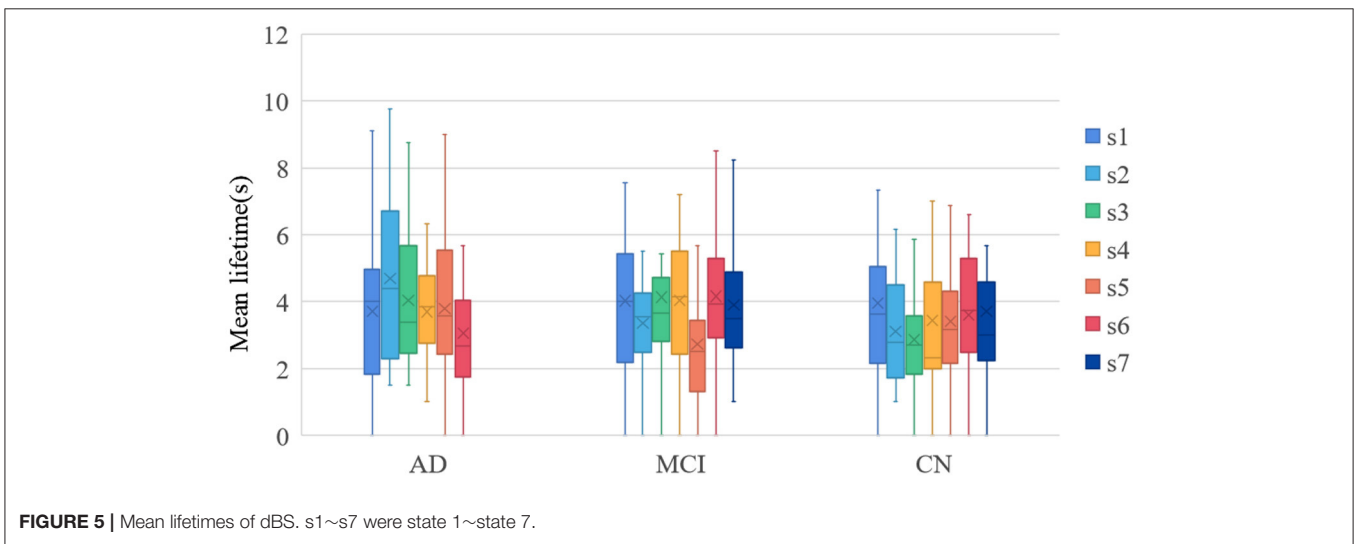
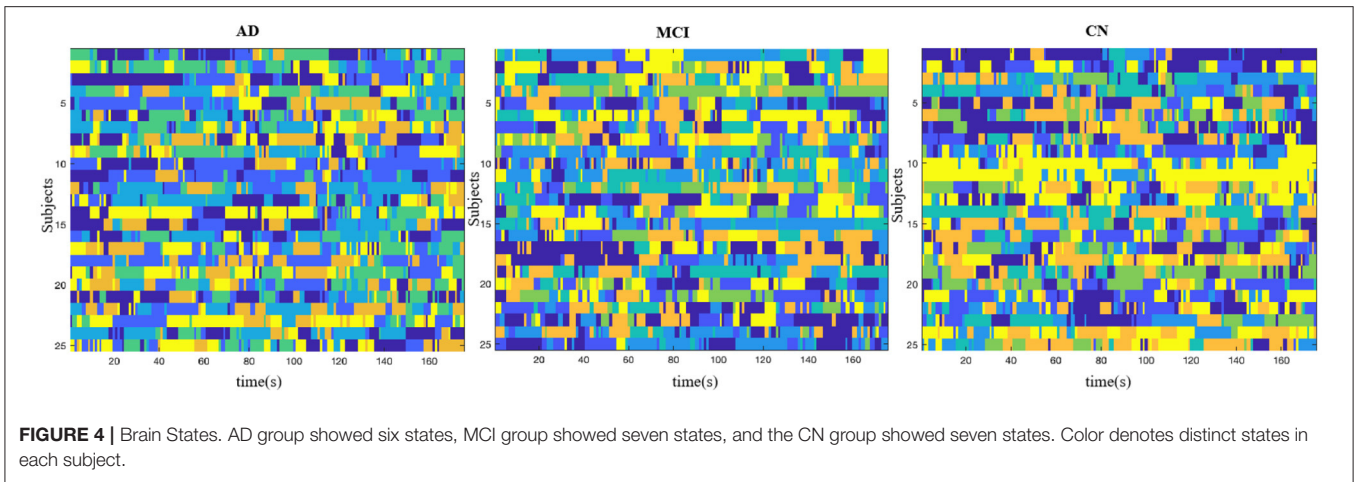
To validation the robustness of differences in dynamic triple-network interactions, we calculated the mean of NII (meanNII) between the three groups. We took meanNII, age, gender as features and used a liner support vector machine (SVM) for classification (39). Due to the limitation of sample size, we applied the leave-one-out cross-validation method to evaluate the performance of the classifier, in order to ensure the reliability and stability of the results. The classification performance was measured by the classification accuracy, precision, recall, and specificity.

RESULTS

Triple-Network in Alzheimer' Disease

Using template multiple regression methods to screen components 18, 29, 25, and 12, we identified four networks SN, DMN, left CEN, and right CEN in Alzheimer' disease. The spatial distribution of components was shown in **Figure 2**.

Since the TR of data was 3 s, the window length was 39 s, that is, 13 time points, and the step size was 1 TR; the data was



187 time points, 175 time windows. The variation of the window weight value w_t with time t was as **Figure 3**.

We examined dynamic cs brain networks identified by the Group ICA and found six states in AD group, seven states in MCI group, and seven states in CN group. Brain States (BS) were shown in **Figure 4**.

Dynamic Triple-Network Interactions

In this study, the mean lifetimes of dynamic Brain States (dBS) were compared of the three groups. Mean lifetimes of dBS were shown in **Figure 5**. From the figure, the mean lifetimes of s2, s3, and s5 in CN group were more significant than in MCI group, but the mean lifetimes of s2 and s5 in AD group were significant than in the MCI group and CN group.

The meanNII in dBS was compared of the three groups. As can be seen from **Figure 6**, the meanNII of the s1, s3, s5 in AD group was more significant than in other groups ($p < 0.05$); the meanNII of the s1, s4 in MCI group was more significant than in CN group ($p < 0.05$).

The Classification Based on Dynamic Triple-Network Interactions in AD

With the meanNII, age and gender as features, SVM was trained in three groups of AD, MCI, and CN. The results of the SVM for the classification were shown in **Table 2**. The method achieved 95% accuracy for distinguishing AD from CN, 94% for AD converters against CN, and 77% for CN converters against MCI.

DISCUSSION

In our work, we aimed to explore the effective dynamic connectivity based a triple-network model in Alzheimer's disease. We identified three large-scale networks (DMN, SN, CEN) important for cognitive control and goal directed behavior in AD (i.e., from CN to MCI to AD) (7, 40). Due to the complexity and unobservable characteristics of brain networks, an indirect method should to be found to explore the network properties of the brain, and the group ICA method provided a feasible means for the study of brain networks. Group ICA estimates the

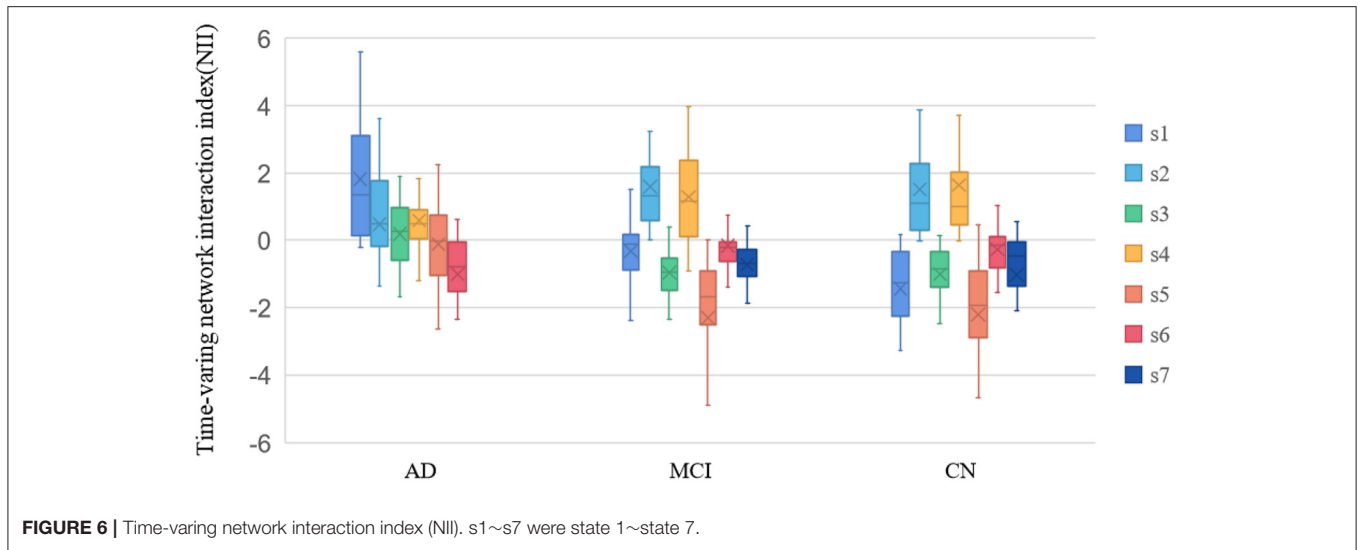


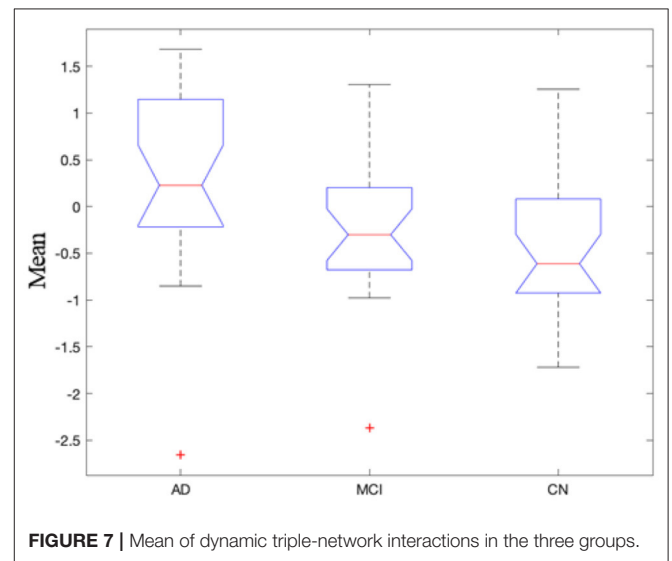
TABLE 2 | Predictive performance of the SVM classifier.

	Accuracy	Precision	Recall	Specificity
AD-CN	0.95	0.93	0.96	0.94
AD-MCI	0.94	0.96	0.91	0.93
CN-MCI	0.77	0.76	0.77	0.76

activation area and time series of each network, and the time series of the network corresponding to the activation area may reflect the dynamics of the network.

As hypothesized, abnormal in AD patients through dynamic functional interactions. Dynamic triple-network coupling measures should predict Alzheimer’s disease (41–43). We found that the dynamic functional network interactions of DMN, CEN, and SN was impaired in AD patients and that these abnormalities conduced to AD. Our findings were consistent with previous studies. Most of the information was directionally transmitted within the DMN, and the anterior default mode network was related to self-referential processing and emotion regulation, and the posterior default mode network was involved in consciousness and memory processing through its relationship with the hippocampus, which indicated plasticity. Information was constantly transformed in cognitive processes such as self-function, emotion, and conscious memory. The SN was involved in the detection and integration of cognitive and emotional information in the brain, indicating that as time progresses, cognitive and emotional information flowed into the SN for processing and integration. The CEN was involved in the regulation of cognitive control processing (19, 44, 45).

In recent years, there were a great deal of evidence of functional connectivity abnormalities inherent in Alzheimer’s disease, but most studied static functional connectivity (46–50). However, there were few studies on dynamic functional connectivity and its relationship with clinical symptoms in Alzheimer’s disease patients (51–53). The mean of NII in the three group (AD, MCI, CN) was analyzed by ANOVA,



the difference was significant ($p = 0.007$). The NII-measured importance of dynamic triple-network interactions in the three groups were $AD > MCI > CN$ (Figure 7). We computed the standard deviations of NII in the three groups ($F = 1.87$). The standard deviation of NII among the three groups was not significantly different ($p = 0.16$). The Pearson correlation analysis of mean NII and MMSE was calculated ($r = 0.281, p = 0.087$). Our findings demonstrated that the dynamic time-varying characteristics of functional interactions between triple-networks contributed to studying the underlying pathophysiology of Alzheimer’s disease, as they captured the dynamic engagement of relevant brain circuits.

To verify the robustness of the findings, we implemented SVM method to examine the extent of differences among AD, MCI, and CN groups in relation to dynamic functional connectivity.

We found that dynamic triple-network interactions have high classification accuracy. This finding indicated that examining the features of dynamic triple-network states may illustrate positive relationships between DMN, SN, and CEN, contributed to understanding Alzheimer's disease.

In summary, our study demonstrated that large-scale functional network dysfunctions in Alzheimer's disease. In the future, studies should be needed to investigate the longitudinal stability of abnormal dynamics in different stages of Alzheimer's disease and to explore whether clinical outcomes differ from DMN, CEN, and SN dysfunction. Analysis of large-scale networks based on triple-networks has showed that they were powerful tools to study the core features of Alzheimer's disease.

DATA AVAILABILITY STATEMENT

Rs-fMRI data were downloaded from the Alzheimer's Disease Neuroimaging Initiative (ADNI) database (<http://adni.loni.usc.edu/>). Application for access to the ADNI data can be submitted by anyone at <http://adni.loni.usc.edu/data-samples/access-data/>. Further enquiries can be directed to the corresponding author.

ETHICS STATEMENT

The ethical review was applied by ADNI. We applied and obtained the access from ADNI. The patients/participants provided their written informed consent to participate in this study. Written informed consent was obtained from the individual(s) for the publication of any potentially identifiable images or data included in this article.

AUTHOR CONTRIBUTIONS

XM, YW, YL, and LM led and supervised the research. XM, YW, and LM designed the research and wrote the article.

REFERENCES

- Villain N, Dubois B. Alzheimer's disease including focal presentations. *Semin Neurol.* (2019) 39:213–26. doi: 10.1055/s-0039-1681041
- Zhong J, Ren X, Liu W, Wang S, Lv Y, Nie L, et al. Discovery of novel markers for identifying cognitive decline using neuron-derived exosomes. *Front Aging Neurosci.* (2021) 13:696944. doi: 10.3389/fnagi.2021.696944
- Jiao Z, Gao P, Ji Y, Shi H. Integration and segregation of dynamic functional connectivity states for mild cognitive impairment revealed by graph theory indicators. *Contrast Media Mol Imaging.* (2021) 2021:6890024. doi: 10.1155/2021/6890024
- Lee ES, Yoo K, Lee YB, Chung J, Lim JE, Yoon B, et al. Default mode network functional connectivity in early and late mild cognitive impairment: results from the Alzheimer's disease neuroimaging initiative. *Alzheimer Dis Assoc Disord.* (2016) 30:289–96. doi: 10.1097/WAD.0000000000000143
- Jiao Z, Zhang J, Shi H, Wu B, Zhang Y. Sparse structure deep network embedding for transforming brain functional network in early mild cognitive impairment classification. *Int J Imaging Syst Technol.* (2021) 31:13. doi: 10.1002/ima.22531
- Ji Y, Zhang Y, Shi H, Jiao Z, Wang SH, Wang C. Constructing dynamic brain functional networks via hyper-graph manifold regularization for mild cognitive impairment classification. *Front Neurosci.* (2021) 15:669345. doi: 10.3389/fnins.2021.669345

XM and DZ performed data pre-processing. XM, YW, and ZX performed triple-network identification. XM, YW, YL, and XY performed independent component analysis, group difference analysis based on k-means clustering and SVM analysis. XM and LM did dynamic triple-network interaction analysis. All authors reviewed, commented, edited, and approved the manuscript.

FUNDING

This study was funded by the National Natural Science Foundation of China (61901063), MOE (Ministry of Education in China) Project of Humanities and Social Sciences (19YJCZH120), Heilongjiang Provincial Natural Science Foundation of China (LH2021H103), Scientific Research Business Fund of Colleges and Universities in Heilongjiang Province (2019-KYYWF-1339), and the Science and Technology Plan Project of Changzhou (CE20205042, CJ20210155, CE20209003). This work was also sponsored by Qing Lan Project of Jiangsu Province. Data collection and sharing for this project was funded by the Alzheimer's Disease Neuroimaging Initiative (ADNI).

ACKNOWLEDGMENTS

Data used in preparation of this article were obtained from the Alzheimer's Disease Neuroimaging Initiative (ADNI) database (adni.loni.usc.edu). As such, the investigators within the ADNI contributed to the design and implementation of ADNI and/or provided data but did not participate in analysis or writing of this report. A complete listing of ADNI investigators can be found at: http://adni.loni.usc.edu/wp-content/uploads/how_to_apply/ADNI_Acknowledgement_List.pdf.

- Supekar K, Cai W, Krishnadas R, Palaniyappan L, Menon V. Dysregulated brain dynamics in a triple-network saliency model of schizophrenia and its relation to psychosis. *Biol Psychiatry.* (2019) 85:60–9. doi: 10.1016/j.biopsych.2018.07.020
- Dennis EL, Thompson PM. Functional brain connectivity using fMRI in aging and Alzheimer's disease. *Neuropsychol Rev.* (2014) 24:49–62. doi: 10.1007/s11065-014-9249-6
- Sridharan D, Levitin DJ, Menon V. A critical role for the right fronto-insular cortex in switching between central-executive and default-mode networks. *Proc Natl Acad Sci USA.* (2008) 105:12569–74. doi: 10.1073/pnas.0800051105
- Borders AJR. Rumination, cognition, and the brain. In: *Borders AJR, editor. Rumination and Related Constructs.* Academic Press (2020). p. 279–311.
- Dong D, Wang Y, Chang X, Luo C, Yao D. Dysfunction of large-scale brain networks in schizophrenia: a meta-analysis of resting-state functional connectivity. *Schizophr Bull.* (2018) 44:168–81. doi: 10.1093/schbul/sbx034
- Zalesky A, Fornito A, Cocchi L, Gollo LL, Breakspear M. Time-resolved resting-state brain networks. *Proc Natl Acad Sci USA.* (2014) 111:10341–6. doi: 10.1073/pnas.1400181111
- Jiao Z, Ji Y, Gao P, Wang S-H. Extraction and analysis of brain functional statuses for early mild cognitive impairment using variational auto-encoder. *J Ambient Intellig Hum Computing.* (2020). doi: 10.1007/s12652-020-02031-w

14. Jiao Z, Ji Y, Jiao T, Wang SJCMiE. Extracting sub-networks from brain functional network using graph regularized nonnegative matrix factorization. *Computer Modeling Eng Sci.* (2020) 123:845–71. doi: 10.32604/cmesci.2020.08999
15. Steimke R, Nomi JS, Calhoun VD, Stelzel C, Paschke LM, Gaschler R, et al. Salience network dynamics underlying successful resistance of temptation. *Soc Cogn Affect Neurosci.* (2017) 12:1928–39. doi: 10.1093/scan/nsx123
16. Anor CJ, O'Connor S, Saund A, Tang-Wai DF, Keren R, Tartaglia MC. Neuropsychiatric symptoms in Alzheimer disease, vascular dementia, and mixed dementia. *Neurodegener Dis.* (2017) 17:127–34. doi: 10.1159/000455127
17. Uddin LQ, Supekar K, Lynch CJ, Khouzam A, Phillips J, Feinstein C, et al. Salience network-based classification and prediction of symptom severity in children with autism. *JAMA Psychiatry.* (2013) 70:869–79. doi: 10.1001/jamapsychiatry.2013.104
18. Jiao Z, Chen S, Shi H, Xu J. Multi-modal feature selection with feature correlation and feature structure fusion for MCI and AD classification. *Brain Sci.* (2022) 12:80. doi: 10.3390/brainsci12010080
19. Menon V. Large-scale brain networks and psychopathology: a unifying triple network model. *Trends Cogn Sci.* (2011) 15:483–506. doi: 10.1016/j.tics.2011.08.003
20. Kronke KM, Wolff M, Shi Y, Kraplin A, Smolka MN, Buhlinger G, et al. Functional connectivity in a triple-network saliency model is associated with real-life self-control. *Neuropsychologia.* (2020) 149:107667. doi: 10.1016/j.neuropsychologia.2020.107667
21. Wu X, Li Q, Yu X, Chen K, Fleisher AS, Guo X, et al. A triple network connectivity study of large-scale brain systems in cognitively normal APOE4 carriers. *Front Aging Neurosci.* (2016) 8:231. doi: 10.3389/fnagi.2016.00231
22. Zhu H, Zhou P, Alcauter S, Chen Y, Cao H, Tian M, et al. Changes of intranetwork and internetwork functional connectivity in Alzheimer's disease and mild cognitive impairment. *J Neural Eng.* (2016) 13:046008. doi: 10.1088/1741-2560/13/4/046008
23. Turner BM, Rodriguez CA, Liu Q, Molloy MF, Hoogendijk M, McClure SM. On the neural and mechanistic bases of self-control. *Cereb Cortex.* (2019) 29:732–50. doi: 10.1093/cercor/bhx355
24. Contreras JA, Avena-Koenigsberger A, Risacher SL, West JD, Tallman E, McDonald BC, et al. Resting state network modularity along the prodromal late onset Alzheimer's disease continuum. *Neuroimage Clin.* (2019) 22:101687. doi: 10.1016/j.nicl.2019.101687
25. Malherbe C, Messé A, Bardinet E, Pélégriani-Issac M, Perlberg V, Marrelec G, et al. Combining spatial independent component analysis with regression to identify the subcortical components of resting-state fMRI functional networks. *Brain Connect.* (2014) 4:181–92. doi: 10.1089/brain.2013.0160
26. Janak PH, Tye KM. From circuits to behaviour in the amygdala. *Nature.* (2015) 517:284–92. doi: 10.1038/nature14188
27. Wang S, Chen B, Yu Y, Yang H, Cui W, Fan G, et al. Altered resting-state functional network connectivity in profound sensorineural hearing loss infants within an early sensitive period: a group ICA study. *Hum Brain Mapp.* (2021) 42:4314–26. doi: 10.1002/hbm.25548
28. Petersen RC, Aisen PS, Beckett LA, Donohue MC, Gamst AC, Harvey DJ, et al. Alzheimer's disease neuroimaging initiative (ADNI): clinical characterization. *Neurology.* (2010) 74:201–9. doi: 10.1212/WNL.0b013e3181cb3e25
29. Filippi M, Spinelli EG, Cividini C, Agosta F. Resting state dynamic functional connectivity in neurodegenerative conditions: a review of magnetic resonance imaging findings. *Front Neurosci.* (2019) 13:657. doi: 10.3389/fnins.2019.00657
30. Izquierdo-Garcia D, Hansen AE, Forster S, Benoit D, Schachoff S, Furst S, et al. An SPM8-based approach for attenuation correction combining segmentation and nonrigid template formation: application to simultaneous PET/MR brain imaging. *J Nucl Med.* (2014) 55:1825–30. doi: 10.2967/jnumed.113.136341
31. Yan CG, Wang XD, Zuo XN, Zang YF. DPABI: Data processing and analysis for (resting-state) brain imaging. *Neuroinformatics.* (2016) 14:339–51. doi: 10.1007/s12021-016-9299-4
32. Calhoun VD, Liu J, Adali T. A review of group ICA for fMRI data and ICA for joint inference of imaging, genetic, and ERP data. *Neuroimage.* (2009) 45(1 Suppl):S163–72. doi: 10.1016/j.neuroimage.2008.10.057
33. Chen S, Ross TJ, Zhan W, Myers CS, Chuang KS, Heishman SJ, et al. Group independent component analysis reveals consistent resting-state networks across multiple sessions. *Brain Res.* (2008) 1239:141–51. doi: 10.1016/j.brainres.2008.08.028
34. Chen T, Cai W, Ryali S, Supekar K, Menon V. Distinct global brain dynamics and spatiotemporal organization of the salience network. *PLoS Biol.* (2016) 14:e1002469. doi: 10.1371/journal.pbio.1002469
35. Ma ZZ, Wu JJ, Hua XY, Zheng MX, Xing XX, Li SS, et al. Tracking whole-brain connectivity dynamics in the resting-state fMRI with post-facial paralysis synkinesis. *Brain Res Bull.* (2021) 173:108–15. doi: 10.1016/j.brainresbull.2021.04.025
36. Steinley D. Profiling local optima in K-means clustering: developing a diagnostic technique. *Psychol Methods.* (2006) 11:178–92. doi: 10.1037/1082-989X.11.2.178
37. Shutaywi M, Kachouie NN. Silhouette analysis for performance evaluation in machine learning with applications to clustering. *Entropy.* (2021) 23:759. doi: 10.3390/e23060759
38. Whitfield-Gabrieli S, Ford JM. Default mode network activity and connectivity in psychopathology. *Annu Rev Clin Psychol.* (2012) 8:49–76. doi: 10.1146/annurev-clinpsy-032511-143049
39. Tkachev V, Sorokin M, Mescheryakov A, Simonov A, Garazha A, Buzdin A, et al. FLOating-window projective separator (FloWPS): a data trimming tool for support vector machines (SVM) to improve robustness of the classifier. *Front Genet.* (2018) 9:717. doi: 10.3389/fgene.2018.00717
40. Yu E, Liao Z, Tan Y, Qiu Y, Zhu J, Han Z, et al. High-sensitivity neuroimaging biomarkers for the identification of amnesic mild cognitive impairment based on resting-state fMRI and a triple network model. *Brain Imaging Behav.* (2019) 13:1–14. doi: 10.1007/s11682-017-9727-6
41. Liang Y, Song C, Liu M, Gong P, Zhou C, Knöpfel T. Cortex-wide dynamics of intrinsic electrical activities: propagating waves and their interactions. *J Neurosci.* (2021) 41:3665–78. doi: 10.1523/JNEUROSCI.0623-20.2021
42. Ballesta-García I, Martínez-González-Moro I, Rubio-Arias J, Carrasco-Poyatos M. High-intensity interval circuit training versus moderate-intensity continuous training on functional ability and body mass index in middle-aged and older women: a randomized controlled trial. *Int J Environ Res Public Health.* (2019) 16:4205. doi: 10.3390/ijerph16214205
43. Reed MJ, Damodarasamy M, Banks WA. The extracellular matrix of the blood-brain barrier: structural and functional roles in health, aging, and Alzheimer's disease. *Tissue Barriers.* (2019) 7:1651157. doi: 10.1080/21688370.2019.1651157
44. Leech R, Sharp DJ. The role of the posterior cingulate cortex in cognition and disease. *Brain J Neurol.* (2014) 137:12–32. doi: 10.1093/brain/awt162
45. Manoliu A, Riedl V, Zherdin A, Mührlau M, Schwerthöffer D, Scherr M, et al. Aberrant dependence of default mode/central executive network interactions on anterior insular salience network activity in schizophrenia. *Schizophr Bull.* (2014) 40:428–37. doi: 10.1093/schbul/sbt037
46. Frisoni GB, Testa C, Zorzan A, Sabatoli F, Beltramello A, Soininen H, et al. Detection of grey matter loss in mild Alzheimer's disease with voxel based morphometry. *J Neurol Neurosurg Psychiatry.* (2002) 73:657–64. doi: 10.1136/jnnp.73.6.657
47. Jalilianhasanpour R, Beheshtian E, Sherbaf G, Sahraian S, Sair HI. Functional connectivity in neurodegenerative disorders: Alzheimer's disease and frontotemporal dementia. *Topics Magn Reson Imaging.* (2019) 28:317–24. doi: 10.1097/RMR.0000000000000223
48. Yamashita KI, Uehara T, Prawiroharjo P, Yamashita K, Togao O, Hiwatashi A, et al. Functional connectivity change between posterior cingulate cortex and ventral attention network relates to the impairment of orientation for time in Alzheimer's disease patients. *Brain Imaging Behav.* (2019) 13:154–61. doi: 10.1007/s11682-018-9860-x
49. Lawrence E, Vegvari C, Ower A, Hadjichrysanthou C, De Wolf F, Anderson RM. A systematic review of longitudinal studies which measure Alzheimer's disease biomarkers. *J Alzheimers Dis.* (2017) 59:1359–79. doi: 10.3233/JAD-170261
50. Penny W, Iglesias-Fuster J, Quiroz YT, Lopera FJ, Bobes MA. Dynamic causal modeling of preclinical autosomal-dominant Alzheimer's disease. *J Alzheimers Dis.* (2018) 65:697–711. doi: 10.3233/JAD-170405

51. Kesika P, Suganthy N, Sivamaruthi BS, Chaiyasut C. Role of gut-brain axis, gut microbial composition, and probiotic intervention in Alzheimer's disease. *Life Sci.* (2021) 264:118627. doi: 10.1016/j.lfs.2020.118627
52. Pchitskaya EI, Zhemkov VA, Bezprozvanny IB. Dynamic microtubules in Alzheimer's disease: association with dendritic spine pathology. *Biochemistry Biokhimiia.* (2018) 83:1068–74. doi: 10.1134/S0006297918090080
53. Zhao Y, Zhao Y, Durongbhan P, Chen L, Liu J, Billings SA, et al. Imaging of nonlinear and dynamic functional brain connectivity based on EEG recordings with the application on the diagnosis of Alzheimer's disease. *IEEE Trans Med Imaging.* (2020) 39:1571–81. doi: 10.1109/TMI.2019.2953584

Conflict of Interest: The authors declare that the research was conducted in the absence of any commercial or financial relationships that could be construed as a potential conflict of interest.

Publisher's Note: All claims expressed in this article are solely those of the authors and do not necessarily represent those of their affiliated organizations, or those of the publisher, the editors and the reviewers. Any product that may be evaluated in this article, or claim that may be made by its manufacturer, is not guaranteed or endorsed by the publisher.

Copyright © 2022 Meng, Wu, Liang, Zhang, Xu, Yang and Meng. This is an open-access article distributed under the terms of the Creative Commons Attribution License (CC BY). The use, distribution or reproduction in other forums is permitted, provided the original author(s) and the copyright owner(s) are credited and that the original publication in this journal is cited, in accordance with accepted academic practice. No use, distribution or reproduction is permitted which does not comply with these terms.